PHYSICAL REVIEW B VOLUME 2, NUMBER 8 15 OCTOBER 1970

Relationship of Surface-State Band Structure to Surface Atomic Configuration of Zinc Blende (110)

J. D. Levine and S. Freeman
RCA Laboratories, Princeton, New Jersey 08540
(Received 16 March 1970)

Intrinsic surface-state band structure has been computed for zinc blende (110) from an adaptation of the Slater-Koster representation of the bulk electronic states. In particular, s orbitals are assigned to the M ions, and p_x, p_y, p_z orbitals to the X ions; the bulk conduction band is then M-like and the valence band is X-like with the correct symmetry. Also, the zone center bandgap and curvature are adjusted to fit experiment or other theory. In this scheme, it has proved possible to explicitly include displacements of M and X surface ions from their ideal positions, consistent with the low-energy electron-diffraction (LEED) result that no reduction of the surface periodicity takes place (no new spots are observed). It was found that both M (acceptor)-like and X (donor)-like surface-state bands appeared most easily when such ion displacements were combined with the modification of the surface "Coulomb integrals" customarily considered. To a first approximation, both M- and X-like surface-state effective masses are found equal to those of the adjoining bulk bands. An analysis such as this is shown to interrelate surface ion geometry with surface electrical properties. In the present case, we find indications that the X (M) ion is displaced into (out of) the nominal surface plane.

I. INTRODUCTION

The (110) surface of zinc blende seems to be an excellent candidate for intrinsic surface-state investigation because (a) this face is the thermally stable cleavage face, so that experimental data on surface states can be readily obtained; (b) this face seems to have no reconstruction[1,2] – there are no new spots on the low-energy electron-diffraction (LEED) pattern; and (c) the crystal face has equal numbers of oppositely charged ions so that different classes of surface states can, and do, simultaneously appear. From a theoretical point of view, there are additional attractive features: (d) The crystal is partly ionic (of the class MX) so that Madelung energies can be used as guides for obtaining surface perturbations[3]; (e) the bulk band gaps are at zone center and direct[4,5] (this simplifies the description of the relevant portion of the energy bands); and (f) the surface atoms are loosely packed and would be expected to rearrange themselves somewhat. We have used a theoretical approach which combines these features, and which can be interrelated with recent experimental measurements of band bending to predict surface atom configurations. Thus, a new diagnostic method is developed. It complements the LEED intensity-versus-energy analysis which has, so far, yielded nonunique surface atom geometrics.

Extrinsic surface states can occur upon adsorption or upon deposition of a foreign oxide or metal; they will not be considered here. The only interface considered is crystal:vacuum.

Koutecký and Tomášek[6] have computed surface-state energy-band extrema for zinc blende, but they considered only the polar (111) and $(\bar{1}\bar{1}\bar{1})$ faces, which are now known to be reconstructed.[1] Their tight-binding model incorporated tetrahedral sp^3 orbitals centered on each M and X site (a total of eight orbitals was used). Only interactions between orbitals on nearest-neighbor (nn) atoms were considered. The resolvent technique was used, as in the present work. In that model, *only one* sp^3 bond need be broken to terminate the $\{111\}$ surfaces, which they presume to be unreconstructed. Jones[7,8] has computed surface-state bands for zinc blende (110); his method involves a truncated pseudopotential, and he terminates the surface by a planar potential-energy discontinuity, matching the wave function only at a single point. His results cannot really be evaluated on the basis of the very brief notes[7,8] published to date. In addition, it is not clear how much relevance a calculation of this type has to real semiconductor crystals, in view of the highly idealized treatment of the surface itself. What, after all, is the significance of this surface discontinuity, and of matching the wave function at a single point? Is this a minor approximation, or does it dominate the results? A less fundamental point of divergence is that Jones does not allow for any sort of lattice distortion in the surface region. Both from our results and from the LEED studies of Si and Ge one would suspect this to be a very serious omission.

The plan in this paper is to start out from a different point of view. That is, a crystal of the form MX is considered to be a collection of M and X ions, to a first approximation. Then only a few orbitals

participate in forming the valence and conduction bands. Thus, the many sophisticated problems of surface termination can be more easily handled. For example, the surface ions are allowed to be in their "ideal" locations, as well as in "displaced" locations, both normal and lateral to the surface plane. The Slater-Koster type of tight-binding quantum theory[9,10] is used, where the bulk band structure and its group symmetries are simulated by having various orbitals located on various locations. A one-dimensional (1-D) treatment of this 3-D model has already been given.[11] It has been pointed out[12] that this type of tight-binding model can better depict the 3-D configurations of the surface region, than the idealization of a planar potential discontinuity at the surface.

Analysis of the above model has been carried out using the resolvent method as well as the ansatz method, both with the aid of a digital computer. A thorough and pedagogically oriented exposition of the resolvent method and its application to this problem is given elsewhere.[13] The resolvent method was the primary method used in this work to achieve numerical results. The ansatz approach was mainly used to independently verify the accuracy of the computational scheme.

The paper is arranged as follows. In Sec. II, the simulated band structure of zinc blende is constructed. The nature of the surface-state wave function is discussed in Sec. III. In Sec. IV, the surface perturbation is defined and our analytic techniques are summarized. The computed surface-state bands are presented in Sec. V. Finally, in Sec. VI, we compare theory with experiment and close with a general discussion.

II. BULK BAND STRUCTURE

The arrangement of ions in the zinc-blende lattice MX is similar to that in the diamond lattice, except that M (cation) and X (anion) ions occupy alternate sites. The crystal structure, as viewed along a $\langle 110 \rangle$ direction, is shown in Fig. 1, both in plan and elevation. The large dark circles are the X ions; the small dark circles are the M ions. The open circles correspond to the layer located behind the first. A reference to M and X as "ions" is convenient, even though the crystal is known to be only partly ionic. Physically, the internuclear spacing is nearly that of the sum of the ionic radii[14]; the (110) surface seems to be stabilized against reconstruction by its lateral electrostatic forces (which are absent in Si and Ge); and the photoelectric threshold is dependent mainly upon the electronegativity of the anion[15] in agreement with simple electrostatic theory.[3] These features, in part, motivated our representation of the zinc-blende band structure which is adapted to the ionic, rather than the covalent, limit.

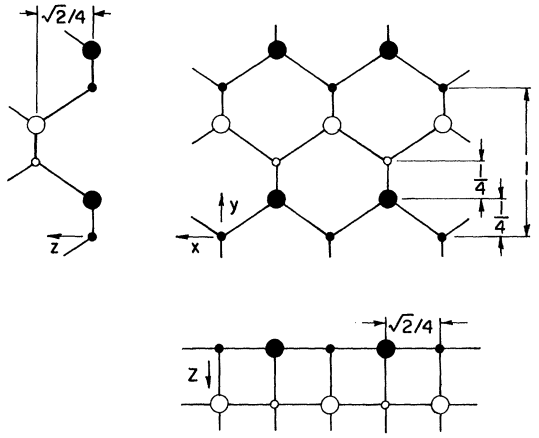

FIG. 1. Plan and elevations of the zinc-blende (110) undistorted atomic structure. Small and large circles represent the M and X ions, respectively. Surface atoms are shown as dark circles. The Bravais lattice of the surface M (or X) sublattice is a rectangle with dimensions $1 \times \frac{1}{2}\sqrt{2}$.

In Fig. 1, a convenient Cartesian coordinate system is introduced. The z direction ([110] on a cube basis) is chosen to be normal to the surface, pointing into the crystal; the x direction points in the direction parallel to the zigzag chains, and the y direction points in the direction (along a cube edge) normal to the chains.

Crystals which have the zinc-blende lattice include ZnS, CdTe, ZnSe, ZnTe, GaAs, and AlSb. The bulk band structure of ZnS (the others are similar) is shown in Fig. 2. It has been theoretically constructed by Walter and Cohen,[5] who used a pseudopotential method with six adjustable form factors (three symmetric and three antisymmetric) and no spin-orbital coupling. The main features of the band structure near the valence–conduction-band gap are (a) the gap occurs at the center Γ of the Brillouin zone (BZ); (b) the conduction-band edge has symmetry Γ_1, and the valence-band edge has a triply degenerate symmetry Γ_{15}; (c) away from zone center, the Γ_{15} level splits into two nearly flat and nearly doubly degenerate heavy hole bands and a light hole band; (d) the band edges are nearly parabolic with values and effective masses (curvatures) which can be inferred from theory or experiment.

All these geometrical (Fig. 1) and band-structure (Fig. 2) features can, in principle, be simulated to any degree of accuracy by assigning $s, p, d, f, \ldots$ "orbitals," as required, to the M and X sites, as basis for a model Hamiltonian. The model Hamiltonian represents the interactions between those localized basis states as transfer integrals between

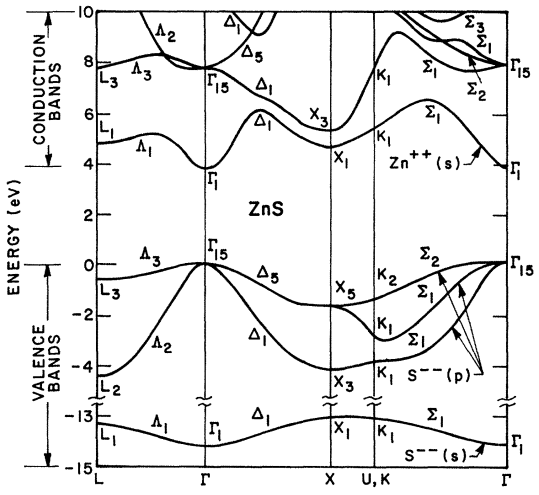

FIG. 2. Bulk band structure of ZnS (from Walter and Cohen, Ref. 5). Simple chemical arguments give the orbitals responsible for the bands, as shown.

orbitals on different neighboring sites. Since our model is designed to simulate a known band structure, rather than to perform an *ab initio* tight-binding calculation, we shall require the various orbitals on different sites to be orthogonal. To solve a complicated surface-state problem, however, it is desirable to use as simple a model as can adequately simulate the band diagram (energy E versus wave vector k) near and within the bandgap region. There is no immediate necessity to attempt to simulate E versus k over the entire energy range $0 < E < 15$ eV in which the bulk band structure[5,9,10,16] is studied; the desired energy range here is more modest, being of the order of the bandgap (~ 5 eV).

The smallest possible number of orbitals necessary to simulate the above features (a)–(d) is four. An s orbital can be placed on the M ion site, and p_x, p_y, p_z orbitals can be placed on the X ion site, in accordance with usual chemical arguments. The set (p_x, p_y, p_z) constitutes a filled spherical subshell; it can be rotated to suit any convenient set of Cartesian coordinates. In the simplest ionic model of ZnS, the Zn^{++} ion has a vacant s orbital, which gives rise to the conduction band, while the S^{--} ion has its p orbitals filled to a subshell of six, and constitutes the valence band. At still lower energy lies the filled S^{--} s orbitals which complete the outer closed shell of eight of the S^{--} orbitals.

A model Hamiltonian based on these s and p orbitals and including only nearest-neighbor interactions in a tight-binding calculation yields the band structure shown in Fig. 3. Comparison of the idealized model in Fig. 3, and the more accurate Fig. 2, shows that the above features (a)–(d) are indeed satisfied, but it is lacking in a number of respects, most significantly, (a) the model (Fig. 3) does not provide the heavy hole valence bands with any curvature – they are unphysically flat, as compared to those in Fig. 2. (b) The covalent limit of this family of compounds cannot be accommodated without either increasing the number of orbitals or their range of interaction. Also, (c) the actual conduction band has subsidiary minima at X_1 and L_1 which are absent in the model. All these defects can be eliminated by adding extra orbitals or more-distant-neighbor interactions, but this enormously increases the labor involved in computing surface states, and will not be attempted here. It is to be emphasized that *no* attempt will be made to compute the bulk bandgap or bulk bandwidth from first principles; instead these will be taken phenomenologically[9,11] from data or other theory.

The localized orbitals will be written in the Dirac notation as $|\vec{n}\nu\rangle$, where $\vec{n}$ is a vector locating the appropriate primitive cell and ν runs from 0 to 3 enumerating the s and p orbitals in the order: s, p_x, p_y, p_z. The vector $\vec{n}$ can be written $\vec{n} = n_1\vec{a} + n_2\vec{b} + n_3\vec{c}$, where $\vec{a}$ and $\vec{b}$ are the nearest like neighbor displacements in the x and y directions, respectively, and $\vec{c}$ extends to a nearest like neighbor displaced in the $+z$ direction (see Fig. 1). For definiteness we choose that neighbor lying in the first quadrant with respect to x and y. Throughout this paper, we shall use the convention that a_0, the cube

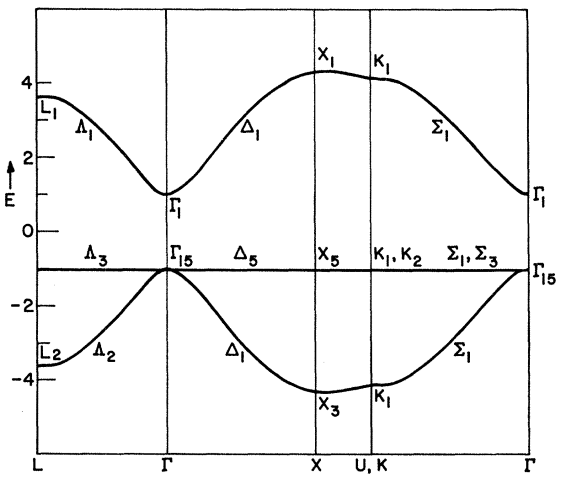

FIG. 3. Bulk band structure of zinc blende as computed by the simplified model used in this paper. This structure has certain features in common with the more accurate structure of Fig. 2. The choice of the zero of the energy scale is simply a matter of convenience. The bandgap and conduction-band curvature can be adjusted to simulate a variety of III-V and II-VI materials.

edge, is of unit length. The localized state symbolized $|\vec{n}\nu\rangle$ is supposed to represent an orthogonalized atomiclike orbital centered on an ion located at the point $\vec{n}+\vec{u}_\nu$. Here $\vec{u}_\nu=0$ for $\nu=0$ (s orbital on cation) and $\vec{u}_\nu=\frac{1}{4}(\sqrt{2},\ 1,\ 0)$ for $\nu=1,\ 2,$ and 3 (p orbitals on anion).

Elements of the bulk Hamiltonian H_0 are defined to include only nearest-neighbor transfer integrals $\langle\vec{n}'\nu'|H_0|\vec{n}\nu\rangle$. These elements are to be determined from known features of the observed band structure such as the magnitude of the bandgap and the curvature of the bands at the Γ point. Diagonal elements $\langle\vec{n}\nu|H_0|\vec{n}\nu\rangle$ are commonly called Coulomb integrals[17] α_M for $\nu=0$ and α_X otherwise. The degeneracy of the three p orbitals is dictated by symmetry, which also implies that there is only one linearly independent off-diagonal element between nearest-neighbor s and p orbitals. This off-diagonal matrix element, or transfer integral, must have the form $\sqrt{3}\beta\cos\Omega$. Here $\sqrt{3}\beta$ is a resonance integral (the factor $\sqrt{3}$ is included for convenience, as will appear below) and Ω is the angle between the line of centers joining the M and X ions and a vector pointing along the positive lobe of the p orbital in question. This vector has been chosen to point in the $+x$, $+y$, or $+z$ coordinate directions for our choice of basis states, as discussed above, and is shown in Fig. 1. For an *undistorted* zinc-blende lattice, the possible values of $\sqrt{3}\beta\cos\Omega$ are $\pm\beta$, $\pm\sqrt{2}\beta$, and 0. More specifically, the vectors which locate the nn X sites from an M site centered at the origin are

$$\vec{n}_1=\tfrac{1}{4}\sqrt{3}\,(\sqrt{\tfrac{2}{3}},\ \sqrt{\tfrac{1}{3}},\ 0)\ ,\quad \vec{n}_3=\tfrac{1}{4}\sqrt{3}\,(0,\ -\sqrt{\tfrac{1}{3}},\ \sqrt{\tfrac{2}{3}})\ , \tag{1}$$

$$\vec{n}_2=\tfrac{1}{4}\sqrt{3}\,(-\sqrt{\tfrac{2}{3}},\ \sqrt{\tfrac{1}{3}},\ 0)\ ,\quad \vec{n}_4=\tfrac{1}{4}\sqrt{3}\,(0,\ -\sqrt{\tfrac{1}{3}},\ -\sqrt{\tfrac{2}{3}})\ .$$

Then the values of $-\cos\Omega$ for transfer from the s orbital to the $(p_x,\ p_y,\ p_z)$ orbitals on one of these four neighboring X sites is just equal to the corresponding triple of direction cosines in (1). Note that $\vec{u}_\nu$ for $\nu=1,\ 2,$ and 3 is just $\vec{n}_1$ according to our choice of primitive cell. The four vectors which join an X site to its nn M sites are just the negative of those in Eq. (1). Thus, for example, $\vec{c}$, defined above, is just $\vec{n}_1-\vec{n}_4$.

The bulk band states are characterized by a conserved wave vector $\vec{k}$. A basis for the states of definite $\vec{k}$ can be defined:

$$|k,\ \nu\rangle=\sum_{\vec{n}}\exp i\vec{k}\cdot(\vec{n}+\vec{u}_\nu)\,|\vec{n},\ \nu\rangle\ . \tag{2a}$$

A complete set of states is obtained by letting ν run from 0 to 3 while $\vec{k}$ ranges over a primitive cell of the reciprocal lattice, which may or may not be chosen to coincide with the first Brillouin zone (FBZ). A convenient choice of this primitive cell will be discussed below.

An eigenstate of H_0, the bulk Hamiltonian, corresponding to some particular k, can be written

$$|\psi\rangle=\sum_{\nu=0}^{3}|\vec{k},\ \nu\rangle\,\gamma_\nu\ . \tag{2b}$$

It must satisfy the Schrödinger equation

$$(H_0-E)\,|\psi\rangle=0\ . \tag{3}$$

Inserting (2a), (2b), and the definition of H_0 into (3), we arrive at the greatly simplified eigenvalue equation:

$$\begin{bmatrix}\alpha_M-E & A_1(\vec{k}) & A_2(\vec{k}) & A_3(\vec{k})\\ A_1(-\vec{k}) & \alpha_X-E & 0 & 0\\ A_2(-\vec{k}) & 0 & \alpha_X-E & 0\\ A_3(-\vec{k}) & 0 & 0 & \alpha_X-E\end{bmatrix}\begin{bmatrix}\gamma_0\\ \gamma_1\\ \gamma_2\\ \gamma_3\end{bmatrix}=0\ , \tag{4}$$

where

$$\begin{bmatrix}A_1(\vec{k})/\beta\\ A_2(\vec{k})/\beta\\ A_3(\vec{k})/\beta\end{bmatrix}=\begin{bmatrix}-\sqrt{2} & \sqrt{2} & 0 & 0\\ -1 & -1 & 1 & 1\\ 0 & 0 & -\sqrt{2} & \sqrt{2}\end{bmatrix}\begin{bmatrix}\exp i\vec{n}_1\cdot\vec{k}\\ \exp i\vec{n}_2\cdot\vec{k}\\ \exp i\vec{n}_3\cdot\vec{k}\\ \exp i\vec{n}_4\cdot\vec{k}\end{bmatrix}. \tag{5}$$

The columns of (5) will be recognized as essentially just the vectors (1). These relations (5) reduce to

$$\begin{aligned}A_1(\vec{k})/\beta&=-2\sqrt{2}\,i\sin\sqrt{\tfrac{1}{8}}k_x\exp i\tfrac{1}{4}k_y\ ,\\ A_2(\vec{k})/\beta&=-2\cos\sqrt{\tfrac{1}{8}}k_x\exp i\tfrac{1}{4}k_y\\ &\quad+2\cos\sqrt{\tfrac{1}{8}}k_z\exp(-i\tfrac{1}{4}k_y)\ ,\\ A_3(\vec{k})/\beta&=-2\sqrt{2}\,i\sin\sqrt{\tfrac{1}{8}}k_z\exp(-i\tfrac{1}{4}k_y)\ ,\end{aligned} \tag{6}$$

and the solution of the secular determinant in (4) yields four energies: the pair

$$\begin{aligned}E=\pm[\Delta^2+4\beta^2(&2\sin^2\sqrt{\tfrac{1}{8}}k_x+2\sin^2\sqrt{\tfrac{1}{8}}k_z+\cos^2\sqrt{\tfrac{1}{8}}k_x\\ &-2\cos\tfrac{1}{8}k_y\cos\sqrt{\tfrac{1}{8}}k_x\cos\sqrt{\tfrac{1}{8}}k_z+\cos^2\sqrt{\tfrac{1}{8}}k_z)]^{1/2}\end{aligned} \tag{7}$$

and a doubly degenerate eigenvalue $E=-\Delta$. Here the following definitions have been used:

$$\alpha_M+\alpha_X=0\ ,\quad \alpha_M-\alpha_X=2\Delta\ . \tag{8}$$

In other words, the energy E will be measured from midgap, and Δ is half the bandgap. The parameter β is seen to be a measure of the bandwidth.

The wave vector, $\vec{k}$, has been expressed in terms of its components in the Cartesian system introduced earlier. It is for this reason that the cubic symmetry of the energy bands is not evident. When the components k_x, k_y, and k_z are reexpressed in terms of the components of $\vec{k}$ along the cube edges,

$$k_x=(k_1+k_2)/\sqrt{2}\ ,\quad k_y=k_3\ ,\quad k_z=(k_1-k_2)/\sqrt{2}\ , \tag{9a}$$

the symmetry of the bands (7) becomes obvious:

$$E=\pm[\Delta^2+16\beta^2(\sin^2\tfrac{1}{4}k_1+\sin^2\tfrac{1}{4}k_2+\sin^2\tfrac{1}{4}k_3$$

$$- \sin^2\tfrac{1}{4}k_1 \sin^2\tfrac{1}{4}k_2 - \sin^2\tfrac{1}{4}k_2 \sin^2\tfrac{1}{4}k_3$$
$$- \sin^2\tfrac{1}{4}k_3 \sin^2\tfrac{1}{4}k_1)]^{1/2} . \qquad (9b)$$

Near zone center and other high symmetry points, one can show that $E(k_1, k_2, k_3)$ has the proper symmetry known to exist for zinc blende.[18,19] However, use of k_x, k_y, and k_z is more convenient in treating the (110) surface states, since it turns out that k_x and k_y are conserved. It remains to define an appropriate and convenient primitive cell for the reciprocal lattice so as to include all distinct states exactly once. The reciprocal lattice consists of all points $m_1\vec{a}^* + m_2\vec{b}^* + m_3\vec{c}^*$, where the starred vectors are the reciprocal basis vectors relative to $\vec{a}$, $\vec{b}$, and $\vec{c}$ in the usual fashion. In terms of the Cartesian basis, they are

$$\vec{a}^* = (\sqrt{2}, 0, -\sqrt{2}) , \quad \vec{b}^* = (0, 1, -\sqrt{2}) , \quad \vec{c}^* = (0, 0, \sqrt{8}) . \qquad (10)$$

A conventional choice for the primitive cell would be a parallelepiped with edges $2\pi\vec{a}^*$, $2\pi\vec{b}^*$, and $2\pi\vec{c}^*$. Note that one edge is already along the z axis and the other two lie in the xz and yz planes, respectively. Making use of the physical equivalence of points displaced relative to one another by $2\pi\vec{c}^*$, we may replace this parallelepiped by a rectangular prism of equal volume having edges parallel to the x, y, and z axes of lengths $2\pi\times\sqrt{2}$, $2\pi\times 1$, and $2\pi\times 1/\sqrt{8}$, respectively. This is the primitive cell which we shall employ.

The bands derived in (7) are illustrated in Fig. 3 for the parameter values: $\Delta = 1$ and $\beta = 1$. This tight-binding band structure seems to be the simplest possible linear combination of atomic orbitals (LCAO) simulation of the actual band structure, Fig. 2. Its main advantage is that it forms a simple, yet somewhat realistic, basis for carrying out the intricate surface state analysis discussed in the next sections.

III. SURFACE-STATE PROPERTIES

Consider a crystal terminated by a (110) surface. We shall eventually take into account displacements of the surface atoms, but none which modify the periodicity of the lattice parallel to the surface plane. The surface is rearranged, but not "reconstructed," in LEED terminology.[1] The lattice vectors $\vec{a}$ and $\vec{b}$ were chosen to lie parallel to the crystal face; they continue to define repeat periods of the crystal. A surface state will be characterized by a two-dimensional (2-D) conserved wave vector parallel to the surface plane. The 2-D reciprocal lattice has basis vectors $2\pi(\sqrt{2}, 0, 0)$ and $2\pi(0, 1, 0)$. These are just the projections of $2\pi\vec{a}^*$ and $2\pi\vec{b}^*$, respectively, parallel to the surface (the xy plane). The corresponding conserved wave-vector components are seen to be just those along the x and y axes. The independent values of k_x and k_y now lie within a 2-D FBZ. This zone is shown in Fig. 4 and is defined $-\pi \le (k_x/\sqrt{2}) \le \pi$, $-\pi \le k_y \le \pi$. The terminology $\bar{\Gamma}$, $\bar{X}$, $\bar{X}'$ has been used by Jones[7,8] to depict a (110) face on an fcc lattice. In forming a surface state of given k_x and k_y, only those bulk states corresponding to the same k_x and k_y can participate. In general, all possible values of k_z will contribute.

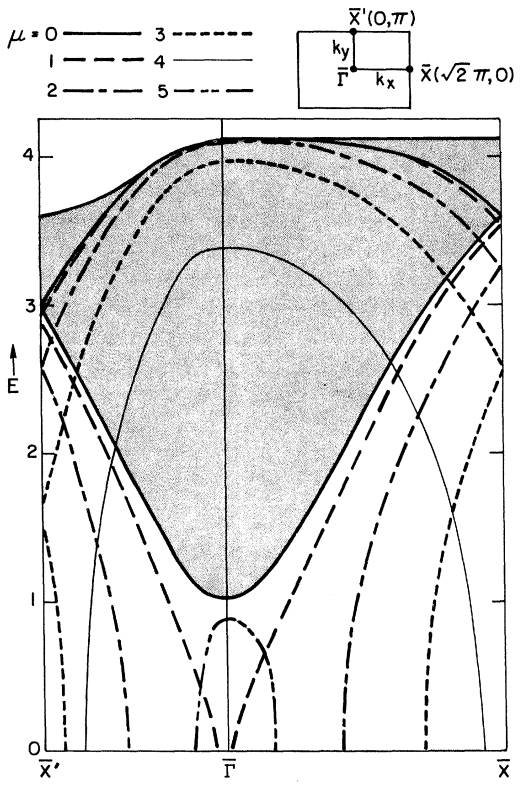

FIG. 4. Analytic continuation according to our model, and 2-D Brillouin zone for zinc blende (110). Each curve is labeled by fixing the damping constant μ, as indicated in the insert. The grey area depicts the energy region of the bulk quasicontinuum, and analytic continuation is not shown above this grey area. The entire figure is symmetrical about midgap, $E = 0$.

Although a surface (bound) state is plane-wave-like in the x and y directions, it is required to be normalizable as far as its dependence on the perpendicular coordinate z is concerned. In order that the wave function fall off away from the surface, it is necessary that the surface-state energy lie outside the energy ranges occupied by bulk states. Here we refer only to bulk states of the same k_x and k_y, of course. On the other hand, in our tight-binding scheme, the influence of the surface on the Hamiltonian H extends only a few lattice planes into the crystal. Expressing the wave function in a po-

sition basis, it is clear that beyond these few lattice planes the equation which the surface state must satisfy is identical to that satisfied by a bulk state. This means that except in the immediate vicinity of the surface, the surface state is a linear combination of bulk states associated with the same E, as well as k_x and k_y. These bulk states behave as damped exponentials as far as k_z is concerned and hence do not represent acceptable eigenstates in the absence of the surface. All such bulk states can be obtained by analytically continuing the relations (4) and (7) to the required E value; this requires complex values of k_z. Note that what is required here is the collection of all possible values of k_z consistent with the given E value, that is, $k_z(E, k_x, k_y)$. This is to be contrasted with the usual end product of a band calculation: $E(k_z, k_x, k_y)$.

When $\vec{k}$ is complex it is no longer true that $A_j(-\vec{k}) = A_j^*(\vec{k})$; thus the matrix in (4) is no longer Hermitian. However, all the relations (1)–(7) retain the same form, nonetheless.

In the present case we shall consider no surface perturbation whose influence extends beyond the first layer of atoms. Then in all subsequent layers the wave function may be expressed as a linear combination of two decaying exponentials. The corresponding complex k_z values

$$k_z = i\mu\ , \qquad k_z = \sqrt{8}\pi + i\mu \tag{11}$$

are obtained from (7). These k_z values represent the only independent ways in which real E values within the gap can be obtained. Here μ_1 and μ_2 are real positive numbers determined from

$$E = \pm\left[\Delta^2 + 4\beta^2(2\sin^2\sqrt{\tfrac{1}{8}}k_x - 2\sinh^2\sqrt{\tfrac{1}{8}}\mu + \cos^2\sqrt{\tfrac{1}{8}}k_x + \cosh^2\sqrt{\tfrac{1}{8}}\mu \mp 2\cos\tfrac{1}{2}k_y\cos\sqrt{\tfrac{1}{8}}k_x\cosh\sqrt{\tfrac{1}{8}}\mu)\right]^{1/2}, \tag{12}$$

where the $-$ and $+$ values inside the square root of (12) correspond to μ_1 and μ_2, respectively. The behavior of the analytically continued relation between k_z and E can best be illustrated graphically, as in Fig. 4. Here the sets $E(k_x, k_y, i\mu_1)$ and $E(k_x, k_y, i\mu_2 + \sqrt{8}\pi)$ are plotted as 2-D bands, depending on k_x and k_y for a succession of fixed values of μ_1 and μ_2. As in Fig. 3, $\Delta = \beta = 1$. The curves are labeled by μ, where $\mu = \mu_1$ or $\mu = \mu_2$ as appropriate. Note that these two families coincide at the zone edge.

Figure 4 suggests rather strongly that the two families of curves $E(k_x, k_y, i\mu)$ and $E(k_x, k_y, i\mu + \sqrt{8}\pi)$ are related to each other by being somehow "folded" at the edge of the 2-D zone. It is instructive to understand the origin of this appearance. It arises because the collection of distinct "bands" of E versus k_x and k_y for fixed complex k_z must be consistent with the periodicity properties of the bulk band structure in $\vec{k}$ space. The 2-D reciprocal lattice has repeat periods in the k_x and k_y directions of magnitude $2\pi\sqrt{2}$ and 2π, respectively, as shown in the insert of Fig. 4. On the other hand, the natural periods of the bulk bands are $2\pi a^*$, $2\pi b^*$, $2\pi c^*$. This remains true for complex k_z. Thus writing $E(k_x, k_y, k_z)$ for the continued bulk energy function, its periodicity properties may be expressed as

$$\begin{aligned} E(k_x, k_y, k_z) &= E(k_x + 2\pi\sqrt{2}, k_y, k_z + \pi\sqrt{8}) \\ &= E(k_x, k_y + 2\pi, k_z + \pi\sqrt{8}) \\ &= E(k_x, k_y, k_z + 2\pi\sqrt{8})\ . \end{aligned} \tag{13}$$

Suppose $E(k_x, k_y, i\mu)$ is real for all k_x and k_y, as is the case for our surface-state problem of interest. Then the first line in (13) implies that a displacement of k_x by $2\pi\sqrt{2}$ in one 2-D "band" $E(k_x, k_y, i\mu)$ leads to another "band" $E(k_x, k_y, i\mu + \pi\sqrt{8})$. Within the 2-D zone these functions are independent. A repetition of the displacement is necessary to return to the original "band." Unfortunately, in general, $E(k_x, k_y, k_z)$ need not be real for *fixed* complex k_z, as k_x and k_y vary. In such a more general case, the implications of (13) are not particularly helpful; in particular, "folding" need not take place [see, for example, Eq. (14) below and the adjoining text].

Understanding the manner in which the bulk bands are folded is helpful when one considers the nature of the wave function arising in this surface-state problem for energies lying in the bulk continuum. As E approaches the conduction-band edge from within the gap, μ_1 goes to zero and then becomes pure imaginary, i.e., the corresponding k_z becomes real. The more slowly decaying exponential is thus replaced by two linearly independent Bloch waves – one incoming and the other outgoing. The faster decaying exponential, having $k_z = i\mu_2 + \sqrt{8}\pi$, varies smoothly in the vicinity of the conduction-band edge. Instead of finding only isolated surface-state solutions for special values of E, Schrödinger's equation can now be solved for *arbitrary* E by adjusting the relative amplitude of the two Bloch waves. As required by (13) the second decaying exponential is associated with the folded extension of the band edge depicted in Fig. 4. As E passes the second "folded" edge, μ_2 goes to zero. Above it, there are two independent states for each E, k_x and k_y. Each is made up of a single incoming Bloch wave and two outgoing Bloch waves. The new incoming Bloch wave has $-k_z$ of the form $q_2 + \sqrt{8}\pi$, where q_2 goes to zero on the folded extension of the band edge. Finally, for E above the conduction band the general solution is a sum of two damped exponentials, with $k_z = \pm\phi + i\mu_3$. Here, E is real only when ϕ and μ_3 satisfy

$$\cos\sqrt{\tfrac{1}{8}}\phi\,\cosh\sqrt{\tfrac{1}{8}}\mu_3 = -\cos\sqrt{\tfrac{1}{8}}k_x\cos\tfrac{1}{2}k_y\ . \tag{14}$$

The band of energies obtained by fixing μ_3 and determining ϕ from (14) is already simply periodic in the 2-D FBZ; relations (13) are irrelevant. We shall not consider the surface states above the conduction band or below the valence band (sometimes called "outer" states[11]). The properties of the bulk states in these regions have been discussed here only for the sake of completeness.

IV. SURFACE-STATE ANALYSIS

Schrödinger's equation for a semi-infinite crystal in the tight-binding approximation takes the form

$$\begin{bmatrix} \underline{W}'-E\underline{I} & \underline{T}_1 & & \\ \underline{T}_2 & \underline{W}-E\underline{I} & \underline{T}_1 & \\ & \underline{T}_2 & \underline{W}-E\underline{I} & \\ & & & \ddots \end{bmatrix} \begin{bmatrix} G_0' \\ G_1 \\ G_2 \\ \vdots \end{bmatrix} \cdot \tag{15}$$

Here H-E is expressed as a matrix array whose entries themselves are 4×4 matrices, dependent on k_x and k_y. Rows and columns of these matrices are labelled by $\nu=0$, 1, 2, 3, in order, and the column eigenvector is given in a comparable form. The nth four-dimensional column vector $\underline{G}_n$ describes a particular layer orbital built up out of the four possible basis states having fixed k_x and k_y and derived exclusively from the orbitals in the nth layer of atoms. The crystal begins with layer zero and is unbounded in the $+z$ direction (increasing n); thus it is unnecessary to consider a second bounding surface. The matirces $\underline{W}$, $\underline{T}_1$, and $\underline{T}_2$ are characteristic of the bulk crystal; they are readily obtained from (4) and (5):

$$\underline{W}=\begin{bmatrix} \alpha_M & A_1(\vec{k}) & -2\beta\cos\sqrt{\tfrac{1}{8}}k_x e^{ik_y/4} & 0 \\ A_1(-\vec{k}) & \alpha_X & 0 & 0 \\ -2\beta\cos\sqrt{\tfrac{1}{8}}k_x e^{ik_y/4} & 0 & \alpha_X & 0 \\ 0 & 0 & 0 & \alpha_X \end{bmatrix},$$

$$\underline{T}_1=\begin{bmatrix} 0 & 0 & \beta e^{ik_y/4} & -\sqrt{2}\,\beta e^{ik_y/4} \\ 0 & 0 & 0 & 0 \\ \beta e^{ik_y/4} & 0 & 0 & 0 \\ \sqrt{2}\,\beta e^{ik_y/4} & 0 & 0 & 0 \end{bmatrix}, \tag{16}$$

and $\underline{T}_2=\underline{T}_1^{\dagger}$.

Here $\underline{W}$ represents interactions within a layer of atoms parallel to the surface, while $\underline{T}_1$ and $\underline{T}_2$ represent interactions between successive layers.

The infinite crystal is terminated by cutting the surface bonds; thus $\underline{T}_2$ is absent in the first row of (15). If the surface region were not affected further, then $\underline{W}'$ would be equal to $\underline{W}$ in (16). This condition is sometimes called the "Shockley condition" because the surface is "unperturbed."[6]

Generally $\underline{W}'\neq\underline{W}$ because of changes in the matrix elements which refer exclusively to the terminal layer; this is the case we shall consider.

In actuality, the surface region should affect other diagonal matrix elements, due to variations in the surface and subsurface electrostatic (Madelung) energies and covalent bond energies, as well as other off-diagonal matrix elements, due to the consequences of the surface and subsurface atom displacements. These will be neglected here, for simplicity.

Suppose that the reflection symmetry possessed by zinc blende (110), as shown in Fig. 1, is unaltered, even in a region of somewhat modified surface atoms. Then the most general possible form of $\underline{W}'$ is

$$\underline{W}'\begin{bmatrix} \alpha_M' & -2\sqrt{2}\,i\beta'\sin\sqrt{\tfrac{1}{8}}k_x e^{ik_y/4} & -2\beta''\cos\sqrt{\tfrac{1}{8}}k_x e^{ik_y/4} & 2\beta'''\cos\sqrt{\tfrac{1}{8}}k_x e^{ik_y/4} \\ 2\sqrt{2}\,i\beta'\sin\sqrt{\tfrac{1}{8}}k_x e^{ik_y/4} & \alpha_x' & 0 & 0 \\ -2\beta''\cos\sqrt{\tfrac{1}{8}}k_x e^{ik_y/4} & 0 & \alpha_y' & \alpha_{yz}' \\ 2\beta'''\cos\sqrt{\tfrac{1}{8}}k_x e^{ik_y/4} & 0 & \alpha_{zy}' & \alpha_z' \end{bmatrix}. \tag{17}$$

For further simplicity, we shall always take

$$\alpha'_x = \alpha'_y = \alpha'_z = \alpha'_X , \quad \alpha'_{yz} = \alpha'_{zy} = 0 . \tag{18}$$

This corresponds to neglecting the changes in the symmetry of the "crystal field" of the surface atoms. Such changes would be expected to split the three otherwise degenerate p orbitals on the surface anion.

The diagonal elements α'_M and α'_X are different from the bulk values α_M and α_X, respectively, because the surface Madelung energy is different from that in the bulk. From simple electrostatic arguments,[3] $\alpha'_M < \alpha_M$ and $\alpha_X < \alpha'_X$. Thus this surface Coulomb perturbation acts in such a way as to attract localized states with energies at the band edges closer to midgap. The values β', β'', β''' in (17) are generally different from β, because bond angles and bond lengths will generally be different for the terminal plane, due to displacements of the atoms. Of course, this effect should also modify the bonds connecting the $n=0$ layer to the next layer $n=1$. As mentioned above, we shall not attempt to include these latter modifications.

Let us consider in detail how the transfer integrals between the surface ions are modified when the ions are displaced relative to one another. Because of our constraints – no reconstruction, retain the reflection symmetry – the possible displacements of the surface ions consist of a uniform displacement of all X ions by a common amount in the yz plane, plus a (generally different) displacement of all M ions in the same plane. Because of the loosely packed structure of zinc blende (110), such displacements seem very plausible.

Assume, for example, that the crystal is characterized by nearest-neighbor bond lengths (links) which are identical and rigid, even in the surface region. Suppose, also, that the *angles* between the links are relatively flexible. This model is based on the fact that the bond energy varies exponentially with the bond length, but only linearly or quadratically with the bond angle. Then the surface sublattices might "rotate," as shown in Fig. 5. Here the zinc-blende M ions are raised above and the X ions are lowered below the nominal surface plane, keeping all the links fixed in length. The figure is drawn for a special rotation angle, $\omega = \omega_0 = 34.9°$. This interesting angle ω_0 is such that the 3 nn cations of a surface anion are coplanar. The M-X-M angles in this planar configuration are 109.5°, 125.25°, 125.25°; this is near to an sp^2 coordination 120°, 120°, 120°. From covalency arguments alone this may be an extra stabilizing feature.[20]

In another example, consider all bond lengths to be fixed (transfer integrals constant) except for those bond lengths which couple one surface atom to another surface atom. A compression (expansion) of this bond causes an increase (decrease) in the resonance integrals. In Fig. 6, such an expansion of the surface atoms is shown. Suppose this bond strength is increased by a factor $(1+\epsilon)$ and there is no rotation ($\omega = 0$). Upon compression, if the bond strength is doubled, $\epsilon = 1$. Upon expansion, if the bond strength is weakened to zero, $\epsilon = -1$.

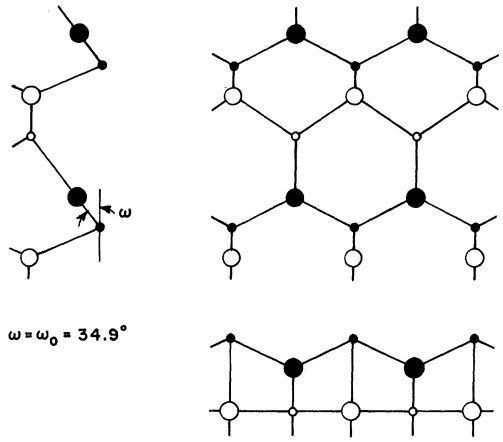

FIG. 5. Geometry of a nonideal surface layer obtained by a rotation of the surface bonds. The rotation is carried out in such a way as to keep all nn bond lengths constant. The angle $\omega_0 = 34.9°$ is such that the X ion is closest to the sp_2 planar coordination.

To superpose and generalize these two effects, recognize that the bond length will change only slightly for relatively large bond energy charges. Thus assume that the surface atoms are rotated as in Fig. 5 (but for arbitrary ω) and that all bond lengths are (effectively) constant. Then, for any compression or expansion (any ϵ) combined with any rotation (and ω), one has the relations

$$\beta' = (1+\epsilon)\beta , \qquad \beta'' = (1+\epsilon)\beta\cos\omega ,$$
$$\beta''' = -(1+\epsilon)\beta\sin\omega . \tag{19}$$

In general, the appearance of an M-like surface state below the conduction-band minimum requires that $\alpha \geq \tau$, where τ is the threshold value of α and $\alpha \equiv \alpha_M - \alpha'_M$. The only combination for which τ vanishes is $\beta'' = \frac{1}{2}\beta$ and $\beta''' = -\frac{1}{2}\beta$; this will be called the "zero threshold condition" for the rest of this paper. Examination of (19) shows that this condition is satisfied whenever $\omega = 54.8°$ (half the tetradedral angle) and $\epsilon = (\sqrt{3}-2)/2 = -0.134$ (slight expansion). We emphasize that neither the rotation nor the expansion changes the periodicity of the M or X surface Bravais lattices, each with dimension $1\times\frac{1}{2}\sqrt{2}$. This means that the LEED pattern should show no new spots, in agreement with experiment.

It remains to solve the eigenvalue problem, defined by (15)–(18), for the surface-state energies.

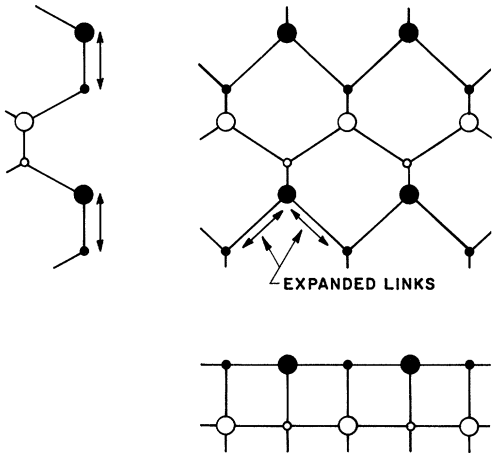

FIG. 6. Another type of nonideal surface obtained by an expansion of the surface bonds. The nn bond lengths between the surface layer and the subsurface layer are kept constant.

The most powerful and general method of treating this type of problem is the resolvent method. This has been described in detail in Ref. 13, where it was applied to the precise problem of interest here. Certain analtyic results, which will be mentioned later, were obtained, and all the necessary preliminaries were carried through to unable us to program a digital computer to obtain the surface-state energies. This has been done, allowing for arbitrary wave vectors k_x and k_y, bulk parameters β and Δ, and surface parameters α_M', α_X', β', β'', and β'''. This program was the primary source of the computed surface-state band structures $E(k_x, k_y)$ presented below.

Before such numerical results can be trusted implicitly, it is necessary to verify the accuracy, both of the algebraic manipulations of Ref. 13 and of the computer program. A number of such checks were mentioned in Ref. 13, but one, in particular – the ansatz method – is properly a part of the present work and will be described here. This method is completely different from the others and was used for spot checks. Agreement was exact. The ansatz method consists in "guessing" the form of the wave function [the column vector in (15)] in terms of a small number of undetermined parameters.[12] After substitution into (15), these parameters and the energies are determined.

How is it possible to determine the right ansatz for the general tight-binding case? The prescription, derived from the resolvent method[13] makes use only of the $\vec{k}$-dependent matrix in (4). Let $2A$ be the *degree* of the determinant of this matrix in e^{iK} after all negative powers of this quantity have been multiplied out. Here K is defined as $K = (\vec{k}\cdot\vec{c}^{\,*})/|\vec{c}^{\,*}|^2$ and is equal to $k_z/\sqrt{8}$ in the present case. (Recall that $\vec{a}$ and $\vec{b}$ lie in the surface plane, so $\vec{c}^{\,*}$ is just a unit vector in the normal direction times the reciprocal of the spacing of successive planes in the z direction.) Similarly let $2B$ be the highest degree of any of the minors of the determinant. We assume $B \geq A$ as in the present case. Suppose that only N surface layers are affected by the surface perturbation [i.e., N rows of columns of (15) are changed from their bulk form]. Then on the first $N+B-A$ layers the wave function has an exceptional form, but otherwise it is a linear combination of A different decaying exponentials, which can be obtained from analytic continuation. In the present case $A=2$, $B=2$, and $N=1$. Thus the general solution is a sum of two decaying exponentials in every layer except the first. The utility of this result is that it reassures us that we have indeed found all decaying exponentials needed to make up the general solution, and that it tells us how many "exceptional" surface layers to allow for.

Consider the multiplication of the matrix and column vector in (15). For every layer (every row) except the first two, the result is simply

$$\underline{W}\,\underline{G}_j + \underline{T}_1\,\underline{G}_{j+1} + \underline{T}_2\,\underline{G}_{j-1} = 0\ , \tag{20}$$

which is identical to (4) as seen most easily be setting $\underline{G}_{j\pm1} = \underline{G}_j\, e^{\pm ik_z/\sqrt{8}}$. Since there are known to be two damped exponentials, one can write, for all $j \geq 1$,

$$\underline{G}_j = \Gamma_a \begin{bmatrix} 1 \\ \gamma_x \\ \\ \gamma_y \\ \gamma_z \end{bmatrix} e^{-(j-1)\mu_1/\sqrt{8}} + \Gamma_b \begin{bmatrix} 1 \\ \gamma_x' \\ \\ \gamma_y' \\ \gamma_z' \end{bmatrix} e^{-(j-1)[(\mu_2/\sqrt{8})+i\pi]} \tag{21}$$

Parameters which are implicit functions of E and which can be obtained by analytic continuation alone are μ_1, μ_2, γ_x, γ_y, γ_z, γ_x', γ_y', and γ_z'. We are left with seven disposable parameters: E, Γ_a, Γ_b, and the four components of G_0'. Of these, one merely is the normalizing constant of the resulting wave function. There are eight linear equations yet to be satisfied, which correspond to the first two rows of (15). However, substitution of (21) in (15) shows that only six of these are linearly independent. This number now matches the number of disposable parameters, and E can be determined. We are assured that such a reduction must take place, in general, since we have used the correct ansatz.

The six independent equations can be written in a matrix equation

$$\begin{matrix} 4\text{ Eqs.} \\ 2\text{ Eqs.} \end{matrix} \left\{ \begin{bmatrix} \underline{W}' - E\underline{I} & \underline{B}_1 \\ \underline{B}_2 & \underline{B}_3 \end{bmatrix} \begin{bmatrix} \underline{G}_0' \\ \Gamma_a \\ \Gamma_b \end{bmatrix} = 0\ . \right. \tag{22}$$

This is no longer an eigenvalue problem of the usual sort for E, since the matrix elements of the rectangular matrices $\underline{B}_1$ and $\underline{B}_2$, as well as the square matrix $\underline{B}_3$, involve complicated functions of E. Surface states are obtained by taking the determinant of the 6×6 matrix in (22). By comparison, a 4×4 matrix[13] is necessary in the resolvent method, but the matrix elements in this case tend to be rather more complicated functions of E. In fact, it can be shown that if one method can be employed, so can the other, and, as we have seen, even the amount of work is about the same.

It should be noted that the "general recipe" for computation of surface states, as given by Wallis, Mills, and Maradudin[21] does not apply here because our bulk 4×4 matrix (4) only allows two energies which depend on wave vector; the other two are the flat bands.

A computed surface state band $E(k_x, k_y)$ is sometimes incomplete in that it exists only over a portion of the 2-D FBZ. At the non-zone-edge limits of region, it encounters one of the bulk band extrema. It is tempting to say that the surface state then "enters" the bulk band and becomes there a virtual state whose width increases as its energy recedes from the bulk band edge. It turns out that this is, in fact, the case in those instances for which we have examined the question (see Fig. 7 and the detailed discussion below).

All wave functions (but not the density of states) of a semi-infinite crystal are affected by the surface, and sometimes a virtual surface state appears. Intuitively, a virtual surface state is an eigenstate in the continuum having a very high relative probability of being found in the surface region. Specifically, we shall consider this probability evaluated for some particular surface layer orbital, summed over all states of energy E, and weighted by the density of states at E. Call this quantity $Q(E)$. A sharp peak in $Q(E)$ will be considered to represent a virtual surface state at that energy, and the lifetime of the resonant state is related in the usual fashion to the reciprocal of the peak width. The quantity $Q(E)$ may be readily obtained from the resolvent formalism (see especially Appendix A of Ref. 13), since it is simply the imaginary part of a matrix element of the resolvent of the interacting system. To study M-like surface states, we define $Q(E)$ in terms of the occupation probability of the surface s orbitals. For the Shockley termination, $Q(E)$ is then just $\mathrm{Im}[R'_{11;00}(E)]$ as given in (86) of Ref. 13. Note that the relation between E and the erstwhile decaying exponentials takes a new form above the band edge. In particular, ik_1 in this formula is now real – no other change need to be made below the "folded extension" of the band edge. Although the methods described in Appendix A of Ref. 13 would permit us to obtain $Q(E)$ for an arbitrary surface perturbation, we have studied it in detail only for an especially simple case: $\alpha'_M \geq \alpha_M$, and α'_X, β', β'', and β''' all have their bulk values. Defining $\alpha \equiv \alpha_M - \alpha'_M$, one finds that $Q = \mathrm{Im}[R'_{11;00}/(1+\alpha R'_{11;00})]$. For $\alpha = -1$, Q is plotted as the ordinate in Fig. 7, for various values of k_x, and for

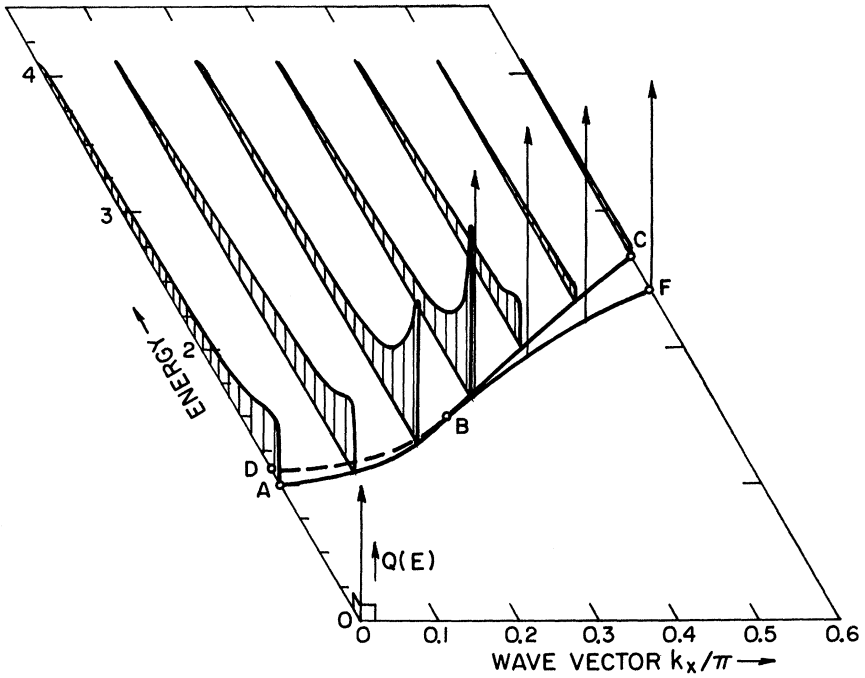

FIG. 7. Plot indicating that a surface-state band (curve BF) is smoothly connected to a scattering resonance (curve DE). The conduction band edge is ABC. $Q(E)$ is the weighted probability of finding a conduction state of energy E on a surface M site (see text).

various energies. Surface state $Q(E)$ functions are δ functions, and are indicated by arrows ↑.

The main result obtained from examining this figure is that the surface-state band (solid curve for $k_x > 0.26\pi$) disappears into the continuum at $k_x/\pi = 0.26$ (large dot) to become what appears to be a virtual state or scattering resonance (dashed curve for $k_x/\pi < 0.26$). As the dashed curve departs further from the band edge, the maximum of $Q(E)$ decreases and the width increases. Eventually, the width can become comparable to the bulk bandwidth, in which case there is no longer any point in speaking of a virtual state.

V. RESULTS

Surface-state bands $E(k_x, k_y)$ in the rectangular BZ of Fig. 4 are computed below for a selected choice of illustrative cases, since there are far too many parameters (α, ϵ, ω, Δ, β) for a more complete parametric analysis. Recall that $\alpha \equiv (\alpha_M - \alpha'_M) = (\alpha'_X - \alpha_X)$, and that the rotation angle ω and the expansion parameter ϵ are related to β', β'', and β''' by (19). Certain special cases are shown in Figs. 8–12. Bulk bands are indicated by the shading; these represent a quasicontinuum of states, each with different k_z in the range $-2\sqrt{2}\pi \leq k_z \leq 2\sqrt{2}\pi$. ($k_z$ is not a good quantum number for the surface states.) The doubly degenerate bulk flat bands at $E = -\Delta$ are not drawn for clarity. If the surface-state bands (solid curves) pass into the bulk quasicontinuum, they may appear as the scattering resonances (dashed curves) described earlier in Fig. 7. In Figs. 8–12, the expected presence of such resonances is indicated schematically by the dashed curves. As found in the cases studied carefully, these resonances become too broad to be meaningful when they recede too far away from the band edge. It is possible that both the surface states and the surface scattering resonances can be observed in certain electrical, optical, and LEED measurements. It should be pointed out that the bulk bands are parabolic at $\bar{\Gamma}$; this parabolic feature is not evident if the $\sqrt{2}$ factor is omitted in a different scale[13] of k_x, k_y.

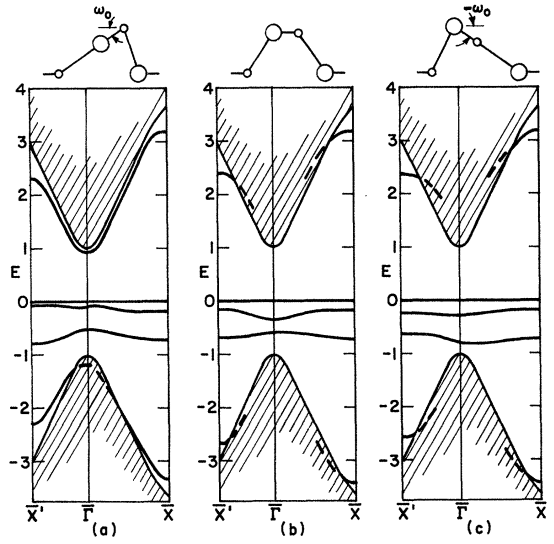

FIG. 8. Effect of rotation of surface bonds through an angle ω. (a) $\omega = \omega_0$, (b) $\omega = 0$, (c) $\omega = -\omega_0$. The M-like surface-state band appears only in (a). In this figure, the dashed curves (scattering resonances) are drawn schematically (not computed). They are only shown close to the band edge, where the resonance is sharp.

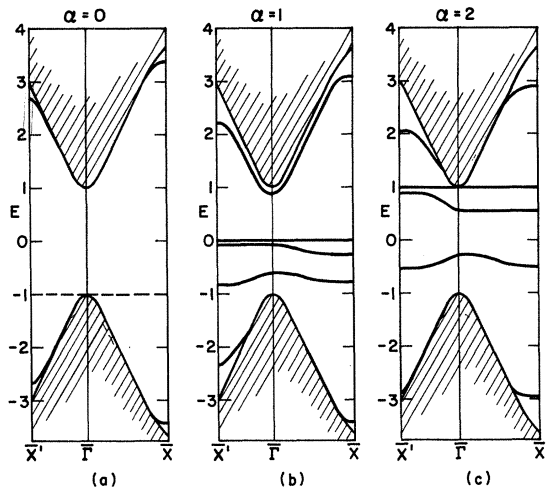

FIG. 9. Effects of Madelung energy difference $\alpha \equiv (\alpha_M - \alpha'_M)$. (a) zero, (b) intermediate, (c) large. $\omega = \omega_0$, $\epsilon = 0$, and the bandgap is fixed.

Two weaknesses of the simplified bulk model of zinc blende have already been mentioned; they are the flat heavy-hole valence bands, and the region in $E(k_x, k_y)$ far from $\bar{\Gamma}$ (zone center). Thus, the surface states which arise either from the flat bands or from the region far away from Γ may be less physically meaningful than those which arise from the parabolic conduction-band minimum (M-like) near Γ. For this reason most emphasis will be given to the M-like surface-state band. Also, there is more data available on the M-like, rather than the X-like, surface states. From the comparison of Figs. 2 and 3, one sees that the ratio $\Delta/\beta = 1$ gives a fair scale mapping of the band structure for ZnS. It will be convenient to assign $\Delta = 1$ and $\beta = 1$ for much of the results below. Effects of varying Δ are considered separately. It will also be convenient to assign $\alpha = 1$ for much of the results below; this corresponds to the surface atom Coulomb integrals having the energy corresponding to midgap; separate variations in α are considered afterwards.

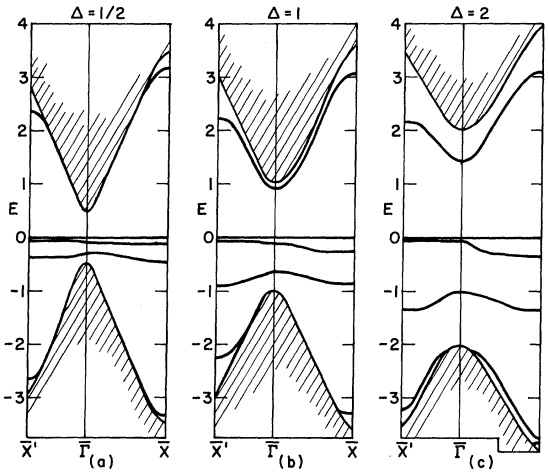

FIG. 10. Effect of variation of the bandgap 2Δ. (a) small, (b) intermediate, (c) large. $\omega = \omega_0$, $\epsilon = 0$, and α/Δ is held fixed.

A. Rotation

Consider first the effects of a surface atom *rotation* as indicated in the structural diagram of Fig. 5 and the $E(k_x, k_y)$ diagrams of Figs. 8(a)–8(c). The parameters fixed here are $\Delta = 1$, $\beta = 1$, $\alpha = 1$, and $\epsilon = 0$. Figure 8(b) has $\omega = 0$ (no movement of surface atoms). Figure 8(a) has $\omega = \omega_0 = 34.9°$ (X ions rotated into sp^2 location as in Fig. 5). Figure 8(c) has $\omega = -34.9°$ (M ions rotated into sp^2 location).

The most significant result of comparing 8(a)–8(c) is that the M-like surface-state band appears below the conduction-band edge only for 8(a). It closely resembles the conduction-band shape and has nearly the same effective mass. (In ZnS at Γ_1 it is isotropic and $m_e^*/m_0 \sim 0.2$). This M-like surface-state band in 8(a) disappears into the quasicontinuum in 8(b) and 8(c). Experimental evidence described later shows that an M-like surface-state band is, in fact, observed, so that case 8(a) seems more probable than 8(b) or 8(c). This is the first known example of a possible correlation between experimental surface-state data (electrical measurements), surface structural data (LEED patterns and atomic geometry), and surface-state theory (computed here). It is evident that such an angular effect will be absent in all one-dimensional treatments appropriate to an MX crystal such as zinc blende,[22–25] and absent in the work of Jones.[7,8]

The next result obtainable from Figs. 8(a)–8(c) is that three X-like surface-state bands appear; these bands are not very sensitive to rotation. The bands have nearly (or exactly) the same effective mass as the flat valence bands from which the upper two arose ($m_h^*/m_0 = \infty$). Data described later indicate that these X-like surface states are also observed. There appears to be no threshold required for these states; the smallest Madelung energy change ($\alpha > 0$) causes them to appear. This feature is certainly exaggerated by our use of perfectly flat valence bands. A realistic picture of the properties of these states clearly requires a more sophisticated model of the bulk band structure. This completes the discussion of how the energy bands vary with surface atom *rotation*.

To determine, for fixed $\omega = \omega_0$, the effect of a change in the surface *Madelung energies*, α is varied in Figs. 9(a)–9(c). In these figures, the quantities kept constant are $\Delta = 1$, $\beta = 1$, $\omega = \omega_0$, and $\epsilon = 0$. Figure 9(b) is identical to Fig. 8(a) with $\alpha = 1$. This is supposed to correspond to a "moderate" Madelung energy perturbation. Case 9(a) corresponds to zero perturbation $\alpha = 0$; and case 9(c) corresponds to a stronger perturbation $\alpha = 2$. Comparing the results of 9(a)–9(c), one finds that the M-like surface-state band is absent in 9(a) because α is less than the threshold value. It is also absent in 9(c) because certain of the X-like surface-state bands have the same symmetry type and repel the M-like state. Of course, the M-like state would appear in 9(c), if $\alpha_M \gg \alpha_M'$ and $\alpha_X' \approx \alpha_X$. Note that in Fig. 9(a) the X-like surface states are triply degenerate and coincide with the bulk flat bands; hence they are shown as dashed lines in the figure.

Variations for fixed $\omega = \omega_0$ of the *bandgap* 2Δ are considered in Fig. 10(a)–10(c). Parameters fixed are $\beta = 1$, $\alpha/\Delta = 1$, $\omega = \omega_0$, $\epsilon = 0$. Figure 10(b) corresponds to Figs. 8(a) and 9(b), where $\Delta = 1$. This is supposed to be a "moderate" bandgap. A smaller bandgap $\Delta = \frac{1}{2}$ with smaller perturbation $\alpha = \frac{1}{2}$ and a

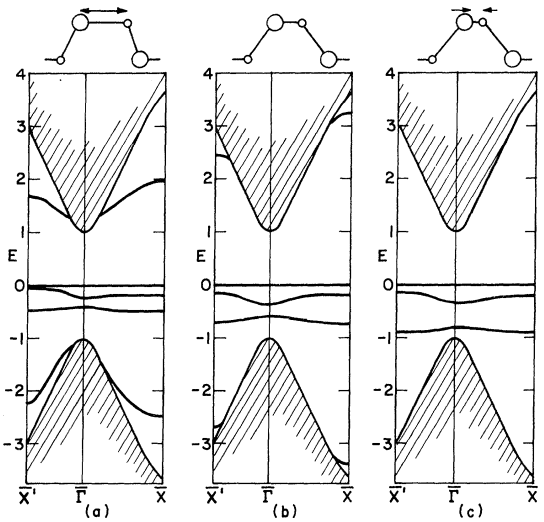

FIG. 11. Effect of variation of the surface bond length. The resonance energy of the bond is multiplied by $(1+\epsilon)$. (a) expansion, represented by $\epsilon = -0.5$; (b) no change, $\epsilon = 0$; (c) compression, $\epsilon = 0.5$. There is no rotation, $\omega = 0$.

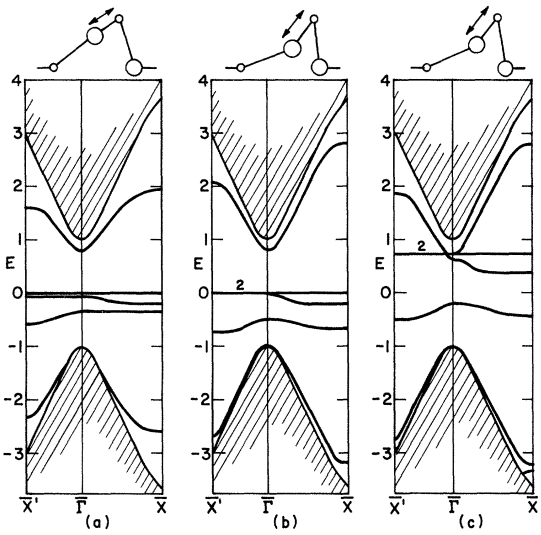

FIG. 12. Combined effects of rotation and expansion. Here $\Delta = 1$. (a) Superposition of $\omega = \omega_0$ and $\epsilon = -0.5$ with $\alpha = 1$. (b) Zero threshold case with $\omega = 54.8°$ = half the tetrahedral angle, and $\epsilon = -0.134$ with $\alpha = 1$. (c) Zero threshold case again, but $\alpha = 1.75$. Note crossing of bands in (c).

larger bandgap $\Delta = 2$ with a larger perturbation $\alpha = 2$ are indicated in Figs. 10(a) and 10(c), respectively. In 10(a) the M-like surface state disappears (as above) because of its proximity to (repulsion by) one of the X-like surface states. In 10(c) it is located proportionally closer to midgap.

At $\bar{X}$ and $\bar{X}'$, above the valence band edge, new X-like surface states appear in Fig. 10(c). These occur only under certain situations [see also Fig. 12(c)]. It is interesting to note that at $\bar{X}$ or $\bar{X}'$ there are as many as six surface-state bands, although only two "dangling bonds" are broken in zinc blende (110).

B. Compression or Expansion

To determine the effects of a surface atom compression and expansion (no rotation), consider the following parameters to be fixed: $\Delta = 1$, $\beta = 1$, $\omega = 0$, and $\alpha = 1$. Figure 11(b) has $\epsilon = 0$ (ideally terminated lattice) and it is identical to Fig. 8(b). Figure 11(a) has $\epsilon = -0.5$, corresponding to halving of the resonance bond energy under expansion. Figure 11(c) has $\epsilon = 0.5$, corresponding to a strengthening of the bond by 50% under compression. The figure shows that in this case expansion makes it easier, and compression makes it harder, to extract the M-like surface-state band. Furthermore, its effective mass is increased (decreased) by the expansion (compression), but it does not appear at $\bar{\Gamma}$ for all the cases considered.

C. Combined Rotation and Expansion

It has been shown above that the appearance of M-like surface states is facilitated by a rotation in the positive sense ($\omega > 0$) and an expansion ($\epsilon < 0$), taken separately. To see if their combined effects are additive, consider $\Delta = 1$, $\beta = 1$, and $\alpha = 1$ to be fixed. In principle, any combination of ω, ϵ will give the desired effect.

As one example, combine the rotation $\omega = \omega_0$ used in Fig. 8(a) and the expansion $\epsilon = -0.5$ used in Fig. 11(a); the combination is shown in Fig. 12(a). Also, consider the zero threshold condition where $\omega = 54.7°$ and $\epsilon = -0.134$, as shown in Fig. 12(b). Figures 12(a) and 12(b) are similar in the sense that they have the additive features of the rotation in Fig. 8(a) (appearance of the M-like state) plus the expansion in Fig. 11(a) (flattening of the M-like surface-state band). No new types of states appear from the combined effects of rotation and compression. A third example, shown in Fig. 12(c) is chosen to demonstrate some M- and X-band crossings possible for certain conditions; this figure is constructed with $\Delta = 1$, $\beta = 1$, $\alpha = 1.75$, $\epsilon = -0.134$, and $\omega = 54.7°$.

Since the above studies in Figs. 8–12 were carried out for limited choices of Δ and α, a more complete cross correlation of these variations is carried out in Figs. 13, 14, and 15. This problem is made tractable by considering the surface-state energies only at zone center. Figure 13 shows how the M- and X-like energies vary as α is increased. This figure shows that as α increases, the M-like surface state first appears below the conduction band after a threshold ($\alpha \geq 0.25$) is reached. Further increase in α increases the trap energy, but a still further increase ($\alpha \geq 2$), decreases it to zero. The repulsion by one of the X-like surface states is clearly indicated in the figure. The upper state enters the conduction band always at $\alpha = 2\Delta$; the middle state

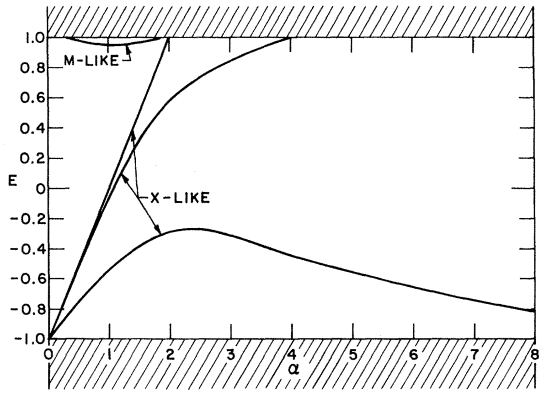

FIG. 13. Surface-state levels at zone center for $\Delta = 1$, $\omega = \omega_0$, $\epsilon = 0$, $\beta = 1$ drawn as a smooth function of Madelung energy difference α.

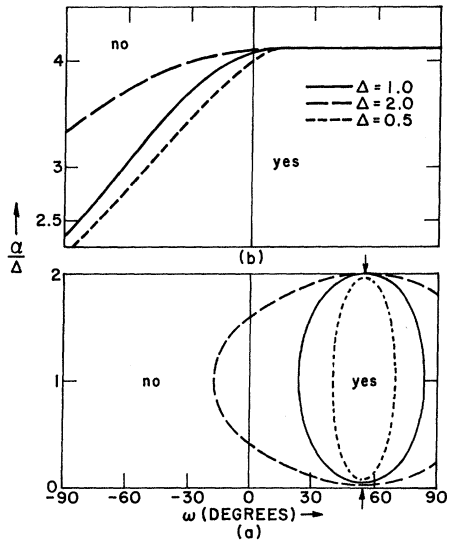

FIG. 14. Existence conditions for (a) the M-like and (b) the second X-like surface state. Dimensionless Madelung energy difference is plotted versus angle of rotation with $\epsilon = 0$. The areas marked "yes" and "no" indicate the existence or nonexistence, respectively, of the surface states.

enters it at a greater value, but the lower state approaches the valence band $-\Delta$ as an asymptote; this last state turns into a subsurface[25] Shockley state in that limit.

That these three X-like surface-state bands really arise from the p orbitals on the surface X ions can be shown as follows. Let $P(X)$ be the probability that an electron occupying a particular surface state will be found on the *surface* X ion. Similarly $P(M)$ is the probability for the surface M ion. Then from Feynman's theorem[26] and the definition of the surface potential-energy perturbation α, it follows that

$$\frac{dE(\alpha)}{d\alpha} = P(X) - P(M) , \tag{23}$$

where $E(\alpha)$ is the energy of the surface state as a function of α, plotted in Fig. 13. From Fig. 13, we see that in the limit $\alpha \to 0$, $dE(\alpha)/d\alpha$ is $+1, +1, +\frac{1}{2}$, for the three X-like surface states. This means that the first two correspond to surface states which are located exclusively on the surface anion (the corresponding surface-state wave functions have no exponential tail), and the third has a probability of being there of at least $\frac{1}{2}$. Since these three states must be orthogonal, the 3 p orbitals involved in these three states must be different. One of the two states with unit probability is easily identified with the p_x orbital (see Fig. 1). The other is "π-like" with respect to the coplanar configuration (see Fig. 5), and it does not interact with the sp^2 planar bonding; it is a linear combination of the p_y and p_z orbitals.

To show the effects of changing ω and Δ (fixing $\epsilon = 0$) it is necessary to further specialize; thus in Fig. 14 the ordinate is α/Δ. The value of this quantity at threshold, where the M-like surface state enters or leaves the conduction band, is written $\tau/\Delta = T$. The abcissa is the angle $-90° \leq \omega \leq 90°$. Each ellipse-shaped curve in Fig. 14(a) has a different bandgap $\Delta = 0.5$, 1.0, and 2.0. First, suppose Δ is given. Then only if the point $(\alpha/\Delta, \omega)$ lies *within* the appropriate ellipse will an M-like surface state exist ("yes" in Fig. 14). Otherwise it will be absent ("no" in Fig. 14). Ellipses (actually near ellipses) are centered about $\omega = 54.7°$. Angles closest to this angle let M-like surface states appear more easily, as shown. Note that none of the ellipses are tangent to $T = 0$; there is always a certain finite threshold $T = 0$ if ϵ is not allowed to vary. It is also shown in Fig. 14(b) that the middle X-like surface state enters the conduction band at $T \geq 2$.

A master plot for fixed $\Delta = 1$ is shown in Fig. 15. Here various contours of constant $T(0.2, 0.5, 1.0)$ are plotted versus ϵ and ω. This diagram shows that a fixed T defines a fixed closed curve. If the point (ϵ, ω) is such as to lie inside the curve, an M-like surface state will exist ("yes" in Fig. 15). The + sign is drawn at the zero threshold point $\omega = 54.7°$, $\epsilon = -0.134$, $T = 0$, which is the center of the near-circular curves. The main result easily obtainable from this figure is that to get an M-like surface state, various combinations and trade offs of (ϵ, ω) can be used. Even for $\omega < 0$, this state is possible provided considerable expansions $\epsilon \approx -1$ are allowed. The limiting case is $\epsilon = -1$, when the surface atoms are far enough expanded so that their bond energy is zero. Alternately, Fig. 15 can be

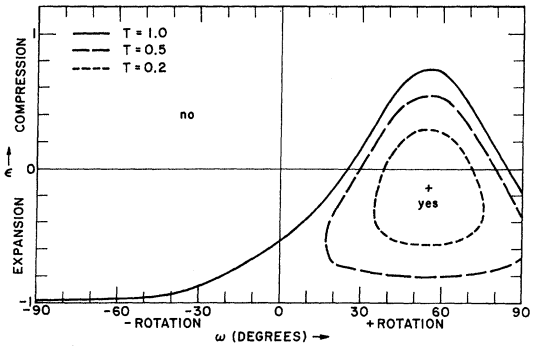

FIG. 15. Existence conditions in a cross-correlated master plot. Contours of constant dimensionless Madelung energy at threshold are plotted versus ϵ and ω. The zero threshold case is labeled by (+) in the figure. The + or − rotations, and the expansions or compressions affect the existence of a surface state in a complicated way, as shown.

thought of as a crude probability diagram. Suppose it is found experimentally that an M-like surface state exists; then it is more likely that it will lie near the centers of the circles. This follows because it is easiest (i.e., smallest T required) to form surface states there.

Certain features of Figs. 8–15 can be summarized as follows:

(i) There are as many as six surface-state bands found. But more frequently, there are five or less, and the ones missing may become scattering resonances (dashed curves).

(ii) The M-like or X-like natures of the surface-state bands can be determined from observing how the bands move with the various perturbations. Figure 13 shows that those nearly flat surface-state bands which arise from the valence band are indeed X-like, as we have frequently implied. For sufficiently small surface perturbations one can argue, from charge neutrality, that these states must be occupied in a neutral crystal. That is, they are normally occupied by electrons at low temperatures and become positively charged when emptied of electrons. Thus they are donorlike states. Alternately they can be called hole traps, since they become positively charged if holes are trapped there.

Similarly, the parabolic surface-state band which arises from the conduction band is M-like. For sufficiently small perturbations, these surface states must be unoccupied in a neutral crystal. They are acceptorlike states; alternately, they can be called electron traps.

For larger perturbations, the origin of the surface states is no longer necessarily correlated with its M- or X-like character (see Fig. 13). Moreover, if a surface-state band crosses another one, or crosses a continuum band edge, its simple donorlike or acceptorlike character may be complicated or even reversed. This would be the case in Fig. 12(c).

(iii) The effective masses of the surface states are similar to the bands from which they arise [again except for Fig. 12(c)]. They are identical in the case $\epsilon = 0$, $\omega = 0$, $E = \Delta$.[13]

(iv) The upper X-like surface state is shown as a horizontal line in all figures. Its energy is $E = \alpha_X'$. It is easy to prive analytically that it should be flat along the line $\bar{\Gamma}$ to $\bar{X}'$ where $k_x = 0$, because $A_1(\vec{k})$ in (16) vanishes and the determinant in (15) has $(E - \alpha_X')$ as a factor. But along the line $\bar{\Gamma} - \bar{X}$ when $k_y = 0$, the flat band is merely a consequence of the degeneracy $\alpha_x' = \alpha_y' = \alpha_z'$ in (18). If this degeneracy is broken, this part of the band is no longer flat. Another type of degeneracy exists in Figs. 12(b) and 12(c); because this is the zero threshold case, all along $\bar{\Gamma} - \bar{X}'$, the two upper X-like surface-state bands are doubly degenerate. This degeneracy is split for ω and ϵ different from those at the zero threshold condition [i.e., Fig. 12(a)].

VI. COMPARISON WITH EXPERIMENT

The intrinsic surface-state properties computed above will now be compared with experiment. Only those experiments will be considered which are characteristic of *clean* zinc-blende surfaces; that is, the surfaces must either be cleaved, or be given the Farnsworth cleaning procedure, while in ultrahigh vacuum $p \ll 10^{-9}$ Torr. Otherwise, the intrinsic surface states can be masked by extrinsic surface states due to adsorbates, oxide formation, etchant residue, etc., or can be chemically passivated.

Theory and experiment are connected through the density of states of the surface-state band and the Fermi statistics. For the M-like parabolic two-dimensional band [e.g., Fig. 12(a)], the density of states is energy independent:

$$\bar{N} = 2 \times 2\pi m_s^*/h^2 \ . \tag{24}$$

Here m_s^* is the effective mass of the surface-state band. From examining Figs. 8–12, m_s^* is nearly the same or somewhat greater than m^* of the bulk conduction band. If the Fermi level E_F lies a few kT below the surface-state band minimum energy E_0, Boltzmann statistics gives for an n-type crystal:

$$Q_{ss}/e = \bar{N}\, kT \exp[\, -(E_0 - E_F)/kT\,] \ , \tag{25}$$

where Q_{ss} is the negative charge (e/cm^{-2}) in this acceptorlike surface-state band; this charge is compensated by the positive charge in an adjacent Schottky depletion layer. From Fig. 12(a), it is seen that $m_s^* > m^*$ for the conduction-band edge. Suppose $m_s^* \sim 2\, m^* = 2 \times 0.1 m_0$, as in CdTe, and suppose $E_0 - E_F = 0.077$ eV at room temperature. Then $\bar{N} = 0.2 \times 4.2 \times 10^{14}\ \mathrm{cm}^{-2}\,\mathrm{eV}^{-1}$, and $Q_{ss}/e = 8.4 \times 10^{13} \times 0.025 \times \exp(-3) = 9 \times 10^{10}\ \mathrm{cm}^{-2}$. This number $9 \times 10^{10}\ \mathrm{cm}^{-2}$ (3×10^{-4} charges per surface cation) is the *observed* number of charges present in the states; it is certainly much less than the number $\sim 10^{15}\ \mathrm{cm}^{-2}$ (~ 1 charge per surface atom) inferred by others[27–29] as an *a priori* condition for the observation of intrinsic surface states. [If the M-like surface-state band would lie entirely inside the bandgap (not seen in Figs. 8–12) and if the Fermi level would lie above this band, only then would a number $\sim 10^{15}\ \mathrm{cm}^{-2}$ be observed.] It will now be shown that $Q_{ss}/e \sim 9 \times 10^{10}\ \mathrm{cm}^{-2}$ is the observed quantity in a typical zinc-blende (110) ultrahigh vacuum experiment, and thus the M-like surface-state parabolic band structure as shown, for example, in Fig. 12(a), 12(b) agrees in this respect with experiment.

The most evidence for intrinsic surface states on zinc blende (110) has come from band-bending studies on cleaved crystals in ultrahigh vacuum.

(Lateral conductivity in the surface-state bands has not been looked for on clean surfaces, and photoemission threshold experiments cannot probe the M-like surface state.) For those zinc-blende (and wurtzite) crystals with partially ionic character and bandgap $E_g > 1$ eV (ZnS, ZnO, ZnSe, CdS, ZnTe, CdSe, AlSb, CdTe, GaAs, InP) it has been shown[30-31] that the $n(p)$-doped crystals have bands which bend up (down) at the surface, in the absence of an applied external field. This is consistent with the $M(X)$-like surface states being called acceptors donors). Consider CdTe as one example. The LEED pattern for CdTe (110) shows no new spots,[2] in agreement with the surface models prepared in Figs. 1, 6, and 7. Swank's photoemission threshold (cube-law extrapolation) and work function measurements[15] on 3 n-type samples,[32] gives $eV_D = 0.23$ eV. By equating the surface-state charge to the Schottky depletion layer charge, it has been shown[31] that the Fermi level is located at $E_0 - E_F = 0.077$ eV. This allows one to compute that $Q_{ss}/e = 9\times10^{10}$ cm^{-2}, as was to be shown, and that $E_{t1} = E_c - E_0 = 0.31$ eV ($E_g = 1.5$ eV). It can be argued that the photoemission threshold determination can possibly be in error by an eV or so because the cube-law extrapolation may not apply. But a separate photovoltage experiment,[15] carried out *in situ* on the same CdTe crystals, showed that $eV_D = 0.29$ eV (differing from 0.23 eV by only 0.06 eV, not ~ 1 eV). See Refs. 30 and 31 for analyses of other zinc blende (110) [and wurtzite ($11\bar{2}0$)] surface-state energies; the results are qualitatively similar to that of CdTe; E_t is a few tenths of an eV for n- and p-type crystals with bandgaps greater than 1 eV.

Having shown that the general shape and the acceptor designation of the M-like parabolic bands are in agreement with experiment, it is desirable to proceed further and to determine E_{t1}, if possible, from theory. To do this, it is necessary to compute the surface-to-bulk Coulomb energy difference $\alpha = \alpha_M - \alpha'_M$. Suppose that α arises solely from the difference between the surface and bulk Madelung energies. Then from classical electrostatics, one has[3]

$$\alpha = ze^2(c_b - c_s)/r \ , \tag{26}$$

where z is the ionic charge or "fractional valence," r is the nn Cd-to-Te distance, c_b is the bulk Madelung coefficient for zinc blende ($c_b = 1.64$), and c_s is the surface Madelung coefficient. Nosker[33] has calculated c_s for zinc blende (110), terminated without surface rearrangement, to be 1.49. For CdTe, $r = 2.78$ Å, and a very crude estimate[3] of z is $\sim\frac{1}{2}$.

A crude estimate of α is then computed from (26) to be $\alpha = 0.4$ eV, whereas the half-bandgap is $\Delta = 0.75$ eV, and the experimentally determined trap depth is 0.31 eV. All that can be safely concluded from the above analysis, at present, is that the magnitude of α seems to be of the order of magnitude of Δ; this choice was used in constructing all of Figs. 8–15. This value may be contrasted to that inferred by Kurtin, McGill, and Mead[34] who concluded in a footnote that α was negligible.

The experimental observation of this M-like surface state with a relatively large trap depth leads one to believe that, most probably, the surface bonds are rotated in the positive direction and expanded, as in Figs. 12(a), 12(b), and the probability chart of Fig. 15.

VII. DISCUSSION

Motivation for a detailed analysis of surface-state bands and their dependences on surface atom geometry has come from recent band-bending measurements[30,31]; these show that M-like intrinsic surface states indeed exist in zinc blende (110), and that they can be accounted for by a parabolic acceptor-like band which has a similar effective mass to that of the bulk conduction band. By interleaving theory and experiment it has been shown in this paper that, most probably, the surface M-X bonds are rotated out of the surface plane with near-constant bond lengths (and perhaps some expansion) to bring the X ion into the crystal and push the M ion farther away.

On the basis of LEED spot asymmetries and spot intensity measurements, MacRae and Gobeli[1] conclude that the surface atoms must be shifted with respect to their ideal locations. Using the Gatos and Lavine[35] dangling band idea, which holds that the M atom (not the X atom as supposed above) prefers a near-sp_2 position, MacRae and Gobeli[1] infer a crude comparison of theory and experiment; but they arbitrarily include a phase factor of $(0.1)\,2\pi$, and no attempt was made to include multiple scattering. Also, they include vertical displacements of magnitude $\pm 0.2/\sqrt{8}a_0$, but ignore lateral displacements, which they concede may well exist.

Other three-dimensional theories of intrinsic surface states[7,8,36,37] involve wave-function matching of a semi-infinite bulk to vacuum at a supposed planar potential discontinuity. It is clear that this approach does not include the possibilities of rotations or expansions of surface bonds, or of changes in the Coulomb energies or in the lateral interactions between surface atoms.

Having shown the types of results obtainable by the above method, it is desirable to point out its main weaknesses; presumably these can be removed in future work. First, the bulk heavy hole valence bands are flat and degenerate as in Fig. 3; they should show dispersion and be nondegenerate as in Fig. 2. In this regard, the theoretical tight-

binding model of Koutecký and Tomášek[6] is no improvement. Second, the transition between the ionic limit and the covalent limit cannot be handled; this can be done somewhat better in their model, and an indirect bandgap can be obtained with appropriate choices of parameters, but they cannot include (without further modifications) the ideal covalent limit of indirect bandgap with ellipsoidal effective masses as in Si, Ge, and diamond. Possibly the more complete and accurate tight-binding model of Kellner[10] is most appropriate. One feature of his model is its inclusion of overlaps.) Some extra flexibility could be obtained in our own model if we considered our orbitals to be true atomic or ionic orbitals, not orthogonal on different sites. An overlap integral σ would then appear in our eigenvalue matrix (4): $(\beta - \sigma E)$ would replace β wherever it appears. Moreover the same substitutions can be made in the final determinantal equation – resolvent or ansatz – provided the E-versus-$\vec{k}$ relation from which the exponents μ_1 and μ_2 are determined is similarly modified. The qualitative consequences of including overlap σ are relatively minor, mainly because there are still two decaying exponentials. Including σ would permit the electron and light hole-effective masses to be different, but it would not rectify the more serious defects of the model enumerated above.

In a larger context, calculation of the effects of the surface should be self-consistent in the senses that (1) the electrostatic effects represented by the surface Madelung constants should be consistent with the actual charge distribution. This latter is affected by charge displacements resulting from the changes in the wave functions in the surface region. (2) The assumed positions of the ion cores in the surface region should, in fact, minimize the surface free energy. It is worth pointing out that the present four-orbital scheme is inadequate for either of these ends. An eight-orbital scheme like that of Kellner or Loutecký and Tomášek is the minimum necessary for either a realistic distribution of the electric charge, or for the inclusion of the directional effects of covalent binding. These latter are presemably dominant in determining the geometry of the surface ion displacements.

In summary, this work represents a start in the direction of correlating surface atom geometry (including the periodicity properties as determined by LEED), with surface electrical measurements (band bending) via a computed surface-state band structure. These correlations indicate that in zinc blende (110) an M-like acceptor surface-state band exists a few tenths of an eV below the conduction band; and the surface bonds are most probably rotated and perhaps expanded. One-dimensional models[22–25] are inadequate to deal with these aspects.

[1]A. U. MacRae, Surface Sci. 4, 247 (1966); see also A. U. MacRae and G. W. Gobeli, in *Semiconductors and Semimetals Vol. 2 Physics of III-V Compounds*, edited by R. K. Willardson and A. C. Beer (Academic, New York, 1966), pp. 115–137.

[2]L. P. Feinstein and D. P. Shoemaker, Surface Sci. 3, 294 (1965). The analogous face for wurtzite, e.g., CdS $(10\bar{1}0)$, also has no new spots. See G. K. Zyrianov and A. T. Hoang, Bull. Leningrad University, Phys. Chem. 2, 73 (1969); and M. F. Chung and H. E. Farnsworth, Surface Sci. 22, 93 (1970).

[3]J. D. Levine and P. Mark, Phys. Rev. 144, 751 (1966).

[4]M. L. Cohen and T. K. Bergstresser, Phys. Rev. 141, 789 (1966).

[5]J. P. Walter and M. L. Cohen, Phys. Rev. 183, 763 (1969).

[6]J. Koutecký and M. Tomášek, Surface Sci. 3, 333 (1965).

[7]R. O. Jones, Phys. Rev. Letters 20, 992 (1968).

[8]R. O. Jones, *The Structure and Chemistry of Solid Surfaces*, edited by G. A. Somorjai (Wiley, New York, 1969), p. 14-1.

[9]J. C. Slater and G. F. Koster, Phys. Rev. 94, 1498 (1954).

[10]Inclusion of overlap integrals was carried out by A. H. Kellner [Acta Physica Austrica 18, 48 (1964) (in English)]; his band structure for diamond is an improvement over that in Ref. 9.

[11]J. D. Levine and S. G. Davison, Phys. Rev. 174, 911 (1968).

[12]J. D. Levine and P. Mark, Phys. Rev. 182, 926 (1969).

[13]S. Freeman, following paper, Phys. Rev. B 2, 3272 (1970).

[14]L. Pauling, *The Nature of the Chemical Bond* (Cornell U. P. Ithaca, 1960), p. 511 ff.

[15]R. K. Swank, Phys. Rev. 153, 844 (1967). It is shown there that the only exception is ZnO (wurtzite).

[16]J. Callaway, *Energy Band Theory* (Academic, New York, 1964).

[17]There is, in fact, a kinetic energy contribution to α_M or α_X.

[18]C. Dresselhaus, A. F. Kip, and C. Kittel, Phys. Rev. 98, 368 (1955).

[19]E. O. Kane, J. Phys. Chem. Solids 1, 249 (1957).

[20]Surface Madelung energy computations involving all nn, nnn, nnnn, ... neighbors have been carried out by R. Nosker (private communication); the most stable *purely electrostatic* configuration is found to be $\omega = 0$.

[21]R. F. Wallis, D. L. Mills, and A. A. Maradudin, in *Localized Excitations in Solids*, edited by R. F. Wallis (Plenum, New York, 1968).

[22]J. D. Levine, Phys. Rev. 171, 701 (1968).

[23]P. Phariseau, Physica 30, 608 (1964).

[24]E. Aerts, Physica 26, 1047 (1960); 26, 1057 (1960); 26, 1063 (1960).

[25]J. Koutecký, Advan. Chem. Phys. 9, 85 (1965).

[26]R. P. Feynman, Phys. Rev. 56, 340 (1939).

[27]A. Many, J. Shappir, and U. Shaked, Surface Sci. 14, 156 (1969).
[28]A. Many, Y. Goldstein, and N. B. Grover, *Semiconductor Surfaces* (North-Holland, Amsterdam, 1965).
[29]D. R. Frankl, *Electrical Properties of Semiconductor Surfaces* (Pergamon, New York, 1967).
[30]J. D. Levine, J. Vac. Sci. Technol. 6, 549 (1969).
[31]S. G. Davison and J. D. Levine, in *Solid State Physics*, edited by H. Ehrenreich, F. Seitz, and D. Turnball (Academic, New York, 1970), Vol. 25, p. 7.
[32]R. K. Swank (private communication).
[33]R. Nosker (private communication).
[34]S. Kurtin, T. C. McGill, and C. A. Mead, Phys. Rev. Letters 22, 1433 (1969).
[35]H. C. Gatos and M. C. Lavine, J. Electrochem. Soc. 107, 433 (1963).
[36]I. Bartoš, Surface Sci. 15, 94 (1969).
[37]C. M. Chaves, N. Majlis, and M. Cardona, Solid State Commun. 4, 271 (1966).

PHYSICAL REVIEW B VOLUME 2, NUMBER 8 15 OCTOBER 1970

Surface States for a Molecular Orbital Model Hamiltonian: Resolvent Methods and Application to Zinc Blende

Smith Freeman
RCA Laboratories, Princeton, New Jersey 08540
(Received 16 March 1970)

A careful discussion is given of the application of the resolvent or Koster-Slater method to a surface-state problem described by a model Hamiltonian of the tight-binding type. Because of a special symmetry, peculiar to the surface-state problem, it is possible to reduce the degree of the characteristic determinant by a factor of 2. The usual, "truncation" method of doing this is shown to sometimes lead to spurious solutions. The origin and properties of these are determined and a prescription for recognizing them presented. An alternative, "pre-severed" approach to the reduction of the determinant is described. This latter is less useful for numerical calculation, but has advantages in obtaining analytical results. The general form of the surface-state wave function is derived from the integral representation of the resolvent. It proves possible to characterize this form using only simple properties of the bulk band structure as represented by the model Hamiltonian. This then permits the popular "ansatz" method of treating the surface states to be routinely used in problems having an arbitrary degree of complexity. The results of the general discussion are applied to determine the surface states associated with the (110) cleavage face of a semiconductor having the zinc-blende structure. The "pre-severed" resolvent method is used to derive some preliminary analytical results, and a program is set up for the numerical calculation of the surface-state properties for more realistic models of the surface perturbation.

I. INTRODUCTION

The (110) face of a II-VI or III-V semiconductor having the zinc-blende structure is an especially interesting surface for theoretical study since it is found experimentally *not* to be reconstructed, i.e., the physical surface retains the full translation symmetry of a parallel bulk plane. This paper, together with its companion work,[1] describes the results of a theoretical investigation of the properties of the electronic surface states associated with such a surface. We have used the molecular orbital (MO) scheme[2] to describe the one-electron states of the crystal and have treated the effects of the surface perturbation via the resolvent technique. This present paper sets up the required formal machinery and applies it to the system of interest. The appropriate matrix elements of the resolvent are here obtained; some results which can be obtained analytically are derived, and the method used in the remaining numerical calculation is outlined. The subsequent paper[1] will display the surface bands derived by numerical calculation for some physically interesting cases. Threshold conditions, which can be obtained by several routes, will be studied there. A discussion will be given there of the physical justification for the particular MO representations chosen to describe the bulk band structure and the surface perturbation, and the results will be compared to experiment.

Section II of the present paper contains a complete and elementary description of the methods used. Various somewhat intricate points, as well as some useful extensions of the basic method which are not required in the present work, are pursued in the appendices. Section III then applies the method to the system of interest. Portions of Sec. II describe methods which are not new and have been used by other authors.[2,7,13,17,18,20,22] However, the central technique used here to obtain the surface electronic states has not been developed or employed before. In addition, the various preliminaries and subordinate techniques characteristic of the surface-state problem, which are usually glossed over, are here